Role of the Dzyaloshinskii-Moriya interaction in multiferroic perovskites

I. A. Sergienko and E. Dagotto

Condensed Matter Sciences Division, Oak Ridge National Laboratory, Oak Ridge, Tennessee 37831, USA
and Department of Physics, The University of Tennessee, Knoxville, Tennessee 37996, USA

With the perovskite multiferroic $R\mathrm{MnO_3}$ ($R = \mathrm{Gd, Tb, Dy}$) as guidance, we argue that the Dzyaloshinskii-Moriya interaction (DMI) provides the microscopic mechanism for the coexistence and strong coupling between ferroelectricity and incommensurate magnetism. We use Monte Carlo simulations and zero-temperature exact calculations to study a model incorporating the double-exchange, superexchange, Jahn-Teller, and DMI terms. The phase diagram contains a multiferroic phase between A and E antiferromagnetic phases, in excellent agreement with experiments.

I. INTRODUCTION

Several recent discoveries of unusually strong coupling between the ferroelectric (FE) and magnetic order parameters have revived interest in the magnetoelectric effect.[1] Due to the possibility of easily controlling the electric properties using magnetic fields, a class of compounds, in which the magnetic order is incommensurate (IC) with the lattice period, is particularly interesting for future applications.[2,3] Surprisingly, this class of multiferroic materials includes compounds with very diverse crystallographic structures: the perovskite $R\mathrm{MnO_3}$ ($R = \mathrm{Gd, Tb, Dy}$),[2,4–8] orthorhombic $R\mathrm{Mn_2O_5}$ ($R = \mathrm{Tb, Ho, Dy}$),[9–13] hexagonal $\mathrm{Ba_{0.5}Sr_{1.5}Zn_2Fe_{12} \times O_{22}}$,[14] and kagomé staircase $\mathrm{Ni_3V_2O_8}$.[15] Unfortunately, the values of the electric polarization achieved so far are two orders of magnitude smaller than those in traditional ferroelectrics. However, it is essential to theoretically understand the new mechanism of magnetoelectric coupling.

Generally, certain types of magnetic order can lower the symmetry of the system to one of the polar groups, which allows for ferroelectricity. This is a central argument of the existing phenomenological models.[7,15,16] According to the recent experimental results in $\mathrm{Ba_{0.5}Sr_{1.5}Zn_2Fe_{12}O_{22}}$,[14] $\mathrm{Ni_3V_2O_8}$,[15] and $\mathrm{TbMnO_3}$,[7] helical magnetic structures are the most likely candidates to host ferroelectricity. In addition, x-ray diffraction studies in a number of the above materials have revealed that the modulated magnetic structure is accompanied by structural modulation.[2,8,11] It is, therefore, a natural assumption that lattice displacements actively participate in the formation of the ferroelectric state as well, even though the FE displacements have not been measured directly, owing to their smallness ($\sim 10^{-3}$ Å, as can be deduced from the value of the FE polarization **P**). This calls for theoretical microscopic models providing a mechanism by which the FE lattice displacements are induced and coupled to the IC magnetic structure.

In this paper, we concentrate on the perovskite manganites since their experimental phase diagram has been studied in much detail.[6,17] We show that the Dzyaloshinksii-Moriya interaction (DMI), linearly dependent on the displacements of the oxygen ions surrounding transition-metal ions, is an essential ingredient in the theory of the magnetoelectric ef-

fect in IC magnets. In independent work,[18] it is suggested that the DMI induces the polarization of the electronic orbitals, without the involvement of the lattice degrees of freedom. In our alternative scenario, the effect of the DMI is twofold: it induces the FE lattice displacements and helps to stabilize helical magnetic structures at low temperature.

II. SEMIEMPIRICAL DISCUSSION

The cubic perovskite structure of $R\mathrm{MnO_3}$ is orthorhombically distorted by the $\mathrm{GdFeO_3}$-type cooperative rotation of the $\mathrm{MnO_6}$ octahedra. Here we use x, y, and z to denote the directions in the pseudocubic setting, and a, b, and c are used for the directions in the orthorhombic structure. The c axis is parallel to z, and the relation between the in-plane axes is shown in Fig. 1(a). In the following, we denote by ICM-FE the phase in which the IC magnetic and FE order coexist. In $R\mathrm{MnO_3}$ ($R = \mathrm{Tb, Dy}$,[2,4,6] and, possibly,[5] Gd), the ICM-FE phase is the ground state. The magnetic structure has the
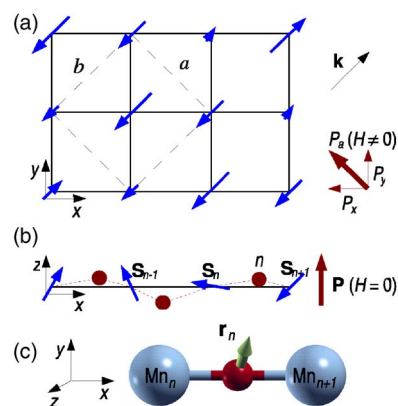

FIG. 1. (Color online) (a), (b) Sketch of the ground-state structure of $\mathrm{TbMnO_3}$. (a) Projection of the Mn spins onto the xy plane. Dashed lines are the boundaries of the unit cell in the orthorhombic setting. The diagram on the right illustrates the emergence of the in-plane component of **P** in applied magnetic field. (b) The zx projection of the spin structure and positions occupied by the O ions (solid circles). (c) The $\mathrm{Mn_2O}$ "molecule" in the cubic perovskite structure. The vector $\mathbf{r}_n$ denotes the displacement of the O ion.

modulation vector **k** along the b axis within the xy plane, and the planes are antiferromagnetically stacked along the z axis. Therefore, for a given Mn ion, the two nearest neighbors in the positive directions of the x and y axes have exactly the same spin, as shown in Fig. 1(a). We use the index n to enumerate the Mn ions along a chain in the x direction [Fig. 1(b)]. According to a neutron diffraction study of TbMnO₃,[7] the classical low-temperature spin structure of the Mn sublattice can be described as[19]

$$S_n^i = S_0^i \cos(n\theta + \alpha_i), \quad (1)$$

where $i = x, y, z$, $S_0^x = S_0^y \approx S_0^z = 1.4$, and $\theta = 0.28\pi$. The experiment was insensitive to the difference between α_x and α_z, but it was found that $\alpha_x = \alpha_y$. This structure is stable for temperatures $T < 28$ K. The lattice structure is also IC with the modulation vector $\mathbf{k}_l = 2\mathbf{k}$.[2] The FE polarization **P** is oriented along the z axis. For 28 K $< T <$ 41 K, another IC, collinear magnetic structure is found with no FE moment.[2,7]

Considering the possible modifications of spin interactions by lattice displacements, we first examine the isotropic superexchange. To address ferroelectricity, we assume that the positions of the Mn ions are fixed, while the O ions can displace from their positions in the paraelectric phase. We consider a chain of Mn ions in the x direction and denote $\mathbf{r}_n = (x_n, y_n, z_n)$ the displacement of the O ion located between the Mn spins $\mathbf{S}_n$ and $\mathbf{S}_{n+1}$ from its position in the idealized cubic perovskite structure. In that structure, the Mn₂O "molecule" shown in Fig. 1(c) has inversion symmetry. Since the symmetric superexchange ($\mathbf{S}_n \cdot \mathbf{S}_{n+1}$) is invariant under inversion (i.e., mere interchange of $\mathbf{S}_n$ and $\mathbf{S}_{n+1}$), this coupling can only depend on even powers of $\mathbf{r}_n$. The axial symmetry of the Mn₂O "molecule" implies

$$H_{\text{ex}} = -\sum_n \left[J_0 + \frac{1}{2} J_\parallel' x_n^2 + \frac{1}{2} J_\perp' (y_n^2 + z_n^2) \right] (\mathbf{S}_n \cdot \mathbf{S}_{n+1}), \quad (2)$$

where J_0, $J_\parallel'$, and $J_\perp'$ are constants and the higher-order terms in $\mathbf{r}_n$ are neglected.

In the actual orthorhombically distorted structure, the oxygen ions are displaced, so that

$$\mathbf{r}_n = (-1)^n \mathbf{r}_0 + \delta\mathbf{r}_n, \quad (3)$$

where $\mathbf{r}_0$ is constant (r_0 is a fraction of 1 Å),[20] and $\delta\mathbf{r}_n$ is the additional displacement, associated with the IC structure (δr_n are of the order of 10^{-3} Å, as mentioned above). It can now be shown that the portion of the Hamiltonian depending on $\delta\mathbf{r}_n$ is

$$\delta H_{\text{ex}} = \sum_n (-1)^{n+1} [J_\parallel' x_0 \delta x_n + J_\perp' (y_0 \delta y_n + z_0 \delta z_n)] (\mathbf{S}_n \cdot \mathbf{S}_{n+1})$$

$$+ H_{\text{el}}, \quad (4)$$

where the elastic energy

$$H_{\text{el}} = \frac{\kappa}{2} \sum_n (\delta x_n^2 + \delta y_n^2 + \delta z_n^2) \quad (5)$$

is assumed isotropic for clarity, the stiffness $\kappa > 0$, and the second-order terms in $\delta\mathbf{r}_n$ are neglected in the magnetoelas-

tic term. Minimizing δH_{ex} with respect to the displacements and using Eq. (1), we obtain

$$\delta z_n = (-1)^n \frac{J_\perp' z_0}{2\kappa} \sum_i S_0^{i2} \{\cos\theta + \cos[(2n+1)\theta + 2\alpha_i]\} \quad (6)$$

and similar expressions for δx_n and δy_n. Hence, this model reproduces the observed structural modulation with the wave vector $2\mathbf{k}$.[2] However, it is insufficient to explain the net FE polarization, since $\sum_n \mathbf{r}_n = 0$ exactly.

On the contrary, the DMI—i.e., anisotropic exchange interaction[21,22] $\mathbf{S}_n \times \mathbf{S}_{n+1}$—changes its sign under inversion. Using group theory, we find that the following expression is invariant under *all* symmetry operations of the MnO₂ "molecule" in the perovskite structure: $\mathbf{D}^{\mathbf{a}}(\mathbf{r}_n) \cdot [\mathbf{S}_n \times \mathbf{S}_{n+1}]$, where

$$\mathbf{D}^{\mathbf{x}}(\mathbf{r}_n) = \gamma(0, -z_n, y_n), \quad \mathbf{D}^{\mathbf{y}}(\mathbf{r}_n) = \gamma(z_n, 0, -x_n) \quad (7)$$

for the Mn-O-Mn bonds along the x and y axes, respectively. The form of Eqs. (7) can also be obtained[23] by perturbative calculations within the Anderson-Moriya theory of superexchange.[22] For the Mn chain in the x direction, the portion of the Hamiltonian depending on $\delta\mathbf{r}_n$,

$$\delta H_{\text{DM}} = \sum_n \mathbf{D}^{\mathbf{x}}(\delta\mathbf{r}_n) \cdot [\mathbf{S}_n \times \mathbf{S}_{n+1}] + H_{\text{el}}, \quad (8)$$

is minimized by

$$\delta z_n = \frac{\gamma}{\kappa} S_0^x S_0^z \sin\theta \sin(\alpha_x - \alpha_z) \quad (9)$$

and $\delta x_n = \delta y_n = 0$. The same result is obtained for the Mn chain in the y direction. Hence, the displacements in this model do not depend on n, leading to a net FE polarization along the z axis. Moreover, Eq. (8) explains why the IC phase with collinear spin structure is paraelectric. Clearly, the equilibrium value of $\delta\mathbf{r}_n$ vanishes in this case.

In applied magnetic fields, the magnetic structure changes through various phase transitions.[6] Thus far, the magnetic structure was only determined experimentally for the magnetic field of 4 T oriented along the a axis.[7] It is similar to the zero-field structure, and it does not induce the in-plane component of **P**.[6] However, as can be seen from Eqs. (7) and (8), the in-plane component of **P** can be induced, in general. It is plausible to assume that the Mn sites that have the same spin at zero field also have the same spin in the applied *uniform* fields [Fig. 1(a)]. Hence, the x component of **P** is always equal in absolute value but opposite in sign to its y component and the in-plane polarization is always directed along the a axis,[24] in agreement with the experiments.[2,6]

Equation (9) allows us to estimate the value of γ. For typical phonon frequencies $\kappa \approx 1$ eV/Å², and we obtain $\gamma \approx 1$ meV/Å. Correspondingly, the magnitude of $\mathbf{D}(\mathbf{r}_n)$ is of the order of $\gamma z_n \approx 0.1$ meV ≈ 1 K, which agrees well with the previous experimental estimations for perovskite manganites.[25–27]

III. STABILIZATION OF THE MAGNETIC HELIX

To further understand the role of the DMI in the stabilization of the ICM-FE phase, we consider the Hamiltonian
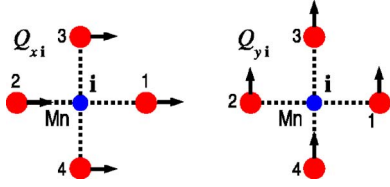
FIG. 2. (Color online) Displacements of oxygen ions (large circles) corresponding to the FE phonon modes in two dimensions.

$$H = - \sum_{\mathbf{i}a\alpha\beta\sigma} t_{\alpha\beta}^{\mathbf{a}} d_{\mathbf{i}\alpha\sigma}^{\dagger} d_{\mathbf{i}+\mathbf{a}\beta\sigma} - J_{\mathrm{H}} \sum_{\mathbf{i}} \mathbf{s_i} \cdot \mathbf{S_i} + J_{\mathrm{AF}} \sum_{\mathbf{i}a} \mathbf{S_i} \cdot \mathbf{S_{i+a}}$$

$$+ \sum_{\mathbf{i}a} \mathbf{D^a(r)} \cdot [\mathbf{S_i} \times \mathbf{S_{i+a}}] + \frac{\kappa_1}{2} \sum_{\mathbf{i}} (Q_{x\mathbf{i}}^2 + Q_{y\mathbf{i}}^2) + H_{\mathrm{JT}}$$

$$+ \frac{\kappa_2}{2} \sum_{\mathbf{i}} \sum_{m} Q_{m\mathbf{i}}^2, \tag{10}$$

based on the orbitally degenerate double-exchange model,[28] for a two-dimensional square lattice, representing a MnO_2 layer, with periodic boundary conditions and one e_g electron per Mn^{3+} ion. Here $d_{\mathbf{i}\alpha\sigma}^{\dagger}$ is the creation operator for the electron on site $\mathbf{i}$, orbital $\alpha = x^2 - y^2(a)$, $3z^2 - r^2(b)$ and carrying spin σ. The hopping integrals are given by $t_{aa}^{x} = -\sqrt{3} t_{ab}^{x} = -\sqrt{3} t_{ba}^{x} = 3 t_{bb}^{x} \equiv t$ and $t_{aa}^{y} = \sqrt{3} t_{ab}^{y} = \sqrt{3} t_{ba}^{y} = 3 t_{bb}^{y} = t$. Hereafter, t is taken as the energy unit. J_{H} is the Hund's coupling constant between the e_g electrons with spin $\mathbf{s_i} = \sum_{\alpha\sigma\sigma'} d_{\mathbf{i}\alpha\sigma}^{\dagger} \boldsymbol{\sigma}_{\sigma\sigma'} d_{\mathbf{i}\alpha\sigma'}$ ($\boldsymbol{\sigma}$ = Pauli matrices) and three t_{2g} electrons treated as a classical three-dimensional spin $\mathbf{S_i}$. In the following, J_{H} is assumed to be infinite. $J_{\mathrm{AF}} > 0$ is the isotropic superexchange constant between the t_{2g} spins. For simplicity, we consider DMI only between the t_{2g} spins and assume that O ions can only move within the plane. $Q_{m\mathbf{i}}$ denote the classical phonon coordinates associated with the displacements of the four O atoms surrounding the Mn site $\mathbf{i}$. The doubly degenerate FE mode $(Q_{x\mathbf{i}}, Q_{y\mathbf{i}})$ is shown in Fig. 2. The Jahn-Teller (JT) interaction term is defined as usual,[28,29]

$$H_{\mathrm{JT}} = \lambda(q_{1\mathbf{i}}\rho_{\mathbf{i}} + q_{2\mathbf{i}}\tau_{x\mathbf{i}} + q_{3\mathbf{i}}\tau_{z\mathbf{i}}) + \frac{1}{2}\sum_{\mathbf{i}} (2q_{1\mathbf{i}}^2 + q_{2\mathbf{i}}^2 + q_{3\mathbf{i}}^2),$$

$$(11)$$

where $\rho_{\mathbf{i}} = \sum_{\alpha\sigma} d_{\mathbf{i}\alpha\sigma}^{\dagger} d_{\mathbf{i}\alpha\sigma}$ and $\tau_{\mathbf{i}} = \sum_{\alpha\beta\sigma} d_{\mathbf{i}\alpha\sigma}^{\dagger} \boldsymbol{\sigma}_{\alpha\beta} d_{\mathbf{i}\beta\sigma}$ is the orbital pseudospin. The three-dimensional JT phonon modes $q_{1,2,3\mathbf{i}}$ have been appropriately redefined for our model in terms of the two-dimensional phonons $Q_{m\mathbf{i}}$.

The remnant phonon modes (not FE or JT) are assumed to have the same spring constant κ_2, an assumption that can be easily removed if necessary. If $\kappa_1 = \kappa_2$, the ICM-FE phase is degenerate with other spin-canted structures. We assume $\kappa_1 < \kappa_2$ in order to lift the degeneracy in favor of the ICM-FE phase.

We have performed extensive Monte Carlo (MC) simulations of H with $\lambda = 0$ on an 8×8 cluster, which is sufficiently large for our purposes. The low-temperature ($T = 0.01$) results are presented in Fig. 3. For small γ, the J_{AF}-γ phase diagram incorporates the FM phase (which is the two-dimensional
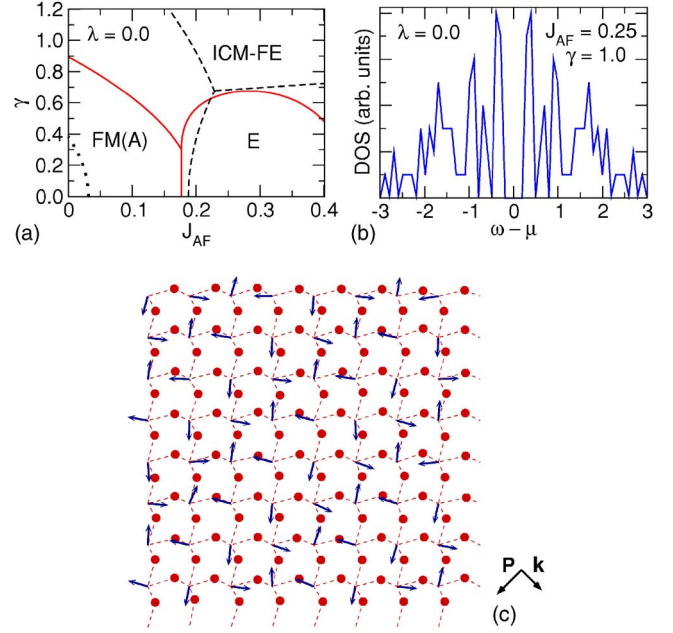

FIG. 3. (Color online) Low-temperature results for model (10) with $\kappa_1 = 1$, $\kappa_2 = 10$. (a) Ground-state phase diagram. Dashed lines are the MC results for the 8×8 cluster. Solid lines are the results of the calculations in the thermodynamic limit. (b) Typical MC electronic density of states (DOS) as a function of the electronic energy ω in the ICM-FE phase. (c) Typical MC snapshot in the ICM-FE phase. Shown are the ICM modulation vector $\mathbf{k}$ and polarization $\mathbf{P}$.

precursor of the three-dimensional A-type antiferromagnetic phase) and the E-type phase, in agreement with previous results for smaller clusters.[29] We find that the FM phase is represented by two states, separated by the dotted line in Fig. 3(a). The regular FM phase with all spins aligned in the same direction is stable on the left-hand side of the dotted line, while the right-hand side is the domain of stability of the so-called "twisted" phase with the period equal to the cluster length. This is a well-known effect of the finite cluster size and periodic boundary conditions.[30–32]

Our most important numerical result is the stabilization of a new modulated (ICM-FE) phase at finite γ. The presence of the three phases in the ground-state phase diagram is in excellent agreement with the experiments.[2,17] The period of the ICM-FE phase is fixed in the MC simulations due to the small cluster, but it is expected to vary smoothly with the parameters of H when the lattice size is increased, as discussed below. A typical snapshot showing the spin structure and O displacements in this phase is presented in Fig. 3(c) showing the spin modulation with $\mathbf{k} = (\pi/2, \pi/2)$. In the two-dimensional model studied here, $\mathbf{P}$ as well as the spins lie within the plane. This is a result of confining the O ions to move within the plane. The ground state with $\mathbf{P}$ along the z direction can be obtained if model (10) is considered in three dimensions and the parameters of the model are changed in accordance with the orthorhombic distortions of the cubic lattice to remove the equivalence of the crystallographic directions.

Figure 3(b) shows the calculated electronic density of states in the ICM-FE phase, with a gap at the chemical po-
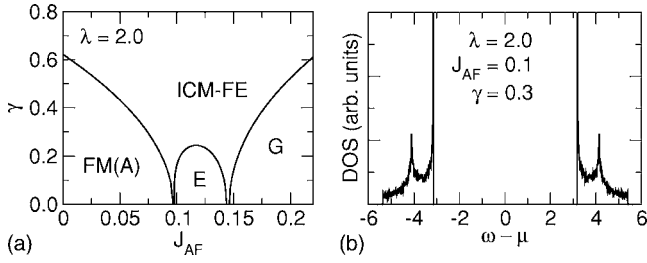
FIG. 4. Results of exact diagnolization of Hamiltonian (10) at $T=0$ in the thermodynamic limit for $\lambda=2.0$, $\kappa_1=1$, and $\kappa_2=10$. (a) Ground-state phase diagram and (b) electronic density of states in the ICM-FE phase.

FIG. 5. (Color online) Finite-temperature MC results for Hamiltonian H; $\kappa_1=1$, $\kappa_2=10$. (a) Typical temperature dependence of the ICM and FE order parameters. The order parameters are normalized to their maximum value at $T=0$. (b) Temperature phase diagram.

tential μ. This demonstrates the insulating character of the new phase, which ensures that the polarization is not screened out by the free charge carriers.

To elucidate the influence of the finite-size effects on the ground-state phase diagram, we calculated the energies for the idealized spin and phonon configurations, for which the e_g part of H can be diagonalized exactly in the thermodynamic limit. This calculation becomes exact at zero temperature for the model considered here, with adiabatic phonons and classical spins, under the reasonable assumption that no other phases appear as ground states. In particular, we obtain for the ICM-FE phase,

$$E_{\text{ICM-FE}} = N\left(-1.60 \cos\frac{\theta}{2} + 2J_{AF}\cos\theta - \frac{\gamma^2}{4\kappa_1}\sin^2\theta\right),$$

(12)

where N is the number of Mn sites in the lattice and θ is the angle between two neighboring spins. As can be seen from Fig. 3(a), while the boundary between the FM and E phases remains practically unchanged, the increase of the lattice size strongly affects the ICM-FE phase. This is expected, since θ can now assume the continuous values found by the minimization of Eq. (12), instead of being restricted by the boundary conditions. Generally, the absolute value of **k** changes from zero at the FM-ICM phase transition to some finite value at the discontinuous ICM-E phase transition. Also, in the phase diagram obtained by this procedure, only the regular FM paraelectric phase is found for small γ and J_{AF} <0.18.

The minimal value of γ needed to stabilize the ICM-FE phase between A and E phases is calculated in the thermodynamic limit to be about 0.3 [see Fig. 3(a)], which corresponds to approximately 200 meV/Å in the physical units. This is two orders of magnitude larger than the expected empirical value obtained in Sec. II. However, the numbers can change as the model is improved. In particular, our zero-temperature results demonstrate that the minimal γ needed can be made infinitesimal if the JT interaction is taken into account. In Fig. 4 we show the results for a realistic value of $\lambda=2.0$. The JT interaction also significantly improves insulating properties of the model. The details of this study for finite λ, including the results on orbital order and MC simulations, will be reported elsewhere.
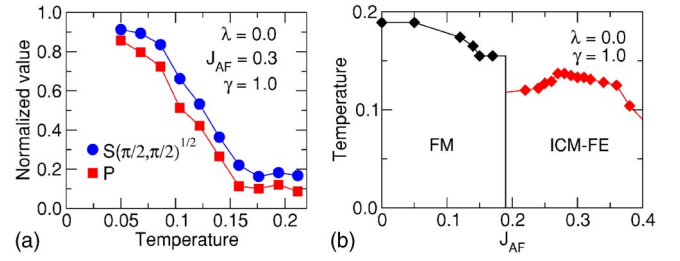
The results of the finite-temperature MC study are reported in Fig. 5. Figure 5(a) depicts a typical temperature dependence of the ICM structure factor and absolute value of **P**. Within the simulation errors, the two order parameters have the same ordering temperature, demonstrating the strong mutual influence of ferroelectricity and magnetic order. The corresponding temperature phase diagram is presented in Fig. 5(b). Here, we find only one ICM phase with a direct phase transition from the disordered state. In order to account for the collinear ICM phase at the intermediate temperatures, one has to include in the model the anisotropy associated with the orthorhombic distortions. Then, different crystallographic axes become inequivalent and the correlations of the corresponding spin components become finite at different temperatures, due to magnetic anisotropy.[33]

IV. CONCLUSIONS

We have demonstrated that the DMI provides a natural explanation for the coexistence and strong coupling between ferroelectricity and IC magnetism in the perovskite manganites. The empirically estimated value of γ is in agreement with previous experiments. The ICM-FE phase appears in the nearest-neighbor interaction model (10) as a result of the competition between the double exchange, superexchange, and DMI. Therefore, our model favors a mechanism of stabilization of helical magnetic order which is qualitatively different from the theories based on spin frustration.[13,17,33] Unlike in the model suggested in Ref. 34 the noncollinear spin state is realized in the *undoped* regime, and thus it is stable with respect to phase separation.[28]

We believe that, due to its universality, the DMI is also relevant in other IC multiferroics. Indeed, the DMI is independent of the orbital structure; it only involves the interaction between spins induced by the symmetry-breaking (in particular FE) ionic displacements. In support of this assertion, we note that, despite the diversity of crystal structures, **P** $\perp$ **k** *always* for all the IC multiferroics discovered so far, with or without applied magnetic field,[2,3,5–7,13–15] which is naturally explained by the DMI.

---

[1] See M. Fiebig, J. Phys. D **38**, R123 (2005) for a recent review.

[2] T. Kimura, T. Goto, H. Shintani, K. Ishizaka, T. Arima, and Y. Tokura, Nature (London) **426**, 55 (2003).

[3] N. Hur, S. Park, P. A. Sharma, J. S. Ahn, S. Guha, and S.-W. Cheong, Nature (London) **429**, 392 (2004).

[4] T. Goto, T. Kimura, G. Lawes, A. P. Ramirez, and Y. Tokura, Phys. Rev. Lett. **92**, 257201 (2004).

[5] K. Noda, S. Nakamura, J. Nagayama, and H. Kuwahara, J. Appl. Phys. **97**, 10C103 (2005).

[6] T. Kimura, G. Lawes, T. Goto, Y. Tokura, and A. P. Ramirez, Phys. Rev. B **71**, 224425 (2005).

[7] M. Kenzelmann, A. B. Harris, S. Jonas, C. Broholm, J. Schefer, S. B. Kim, C. L. Zhang, S.-W. Cheong, O. P. Vajk, and J. W. Lynn, Phys. Rev. Lett. **95**, 087206 (2005).

[8] T. Arima, T. Goto, Y. Yamasaki, S. Miyasaka, K. Ishii, M. Tsubota, T. Inami, Y. Murakami, and Y. Tokura, Phys. Rev. B **72**, 100102(R) (2005).

[9] N. Hur, S. Park, P. A. Sharma, S. Guha, and S.-W. Cheong, Phys. Rev. Lett. **93**, 107207 (2004).

[10] L. C. Chapon, G. R. Blake, M. J. Gutmann, S. Park, N. Hur, P. G. Radaelli, and S.-W. Cheong, Phys. Rev. Lett. **93**, 177402 (2004).

[11] D. Higashiyama, S. Miyasaka, N. Kida, T. Arima, and Y. Tokura, Phys. Rev. B **70**, 174405 (2004).

[12] S. Kobayashi, T. Osawa, H. Kimura, Y. Noda, N. Kasahara, S. Mitsuda, and K. Kohn, J. Phys. Soc. Jpn. **73**, 3439 (2004).

[13] G. R. Blake, L. C. Chapon, P. G. Radaelli, S. Park, N. Hur, S.-W. Cheong, and J. Rodríguez-Carvajal, Phys. Rev. B **71**, 214402 (2005).

[14] T. Kimura, G. Lawes, and A. P. Ramirez, Phys. Rev. Lett. **94**, 137201 (2005).

[15] G. Lawes, A. B. Harris, T. Kimura, N. Rogado, R. J. Cava, A. Aharony, O. Entin-Wohlman, T. Yildrim, M. Kenzelmann, C. Broholm, and A. P. Ramirez, Phys. Rev. Lett. **95**, 087205(R) (2005).

[16] V. G. Bar'yakhtar, V. A. L'vov, and D. A. Yablonskii, Pis'ma Zh. Eksp. Teor. Fiz. **37**, 565 (1983) [JETP Lett. **37**, 673 (1983)].

[17] T. Kimura, S. Ishihara, H. Shintani, T. Arima, K. T. Takahashi, K. Ishizaka, and Y. Tokura, Phys. Rev. B **68**, 060403(R) (2003).

[18] H. Katsura, N. Nagaosa, and A. V. Balatsky, Phys. Rev. Lett. **95**, 057205 (2005).

[19] Here, we do not consider the magnetic moments of the rare-earth ions explicitly, since they are not directly related to the FE order.

[20] J. Blasco, C. Ritter, J. García, J. M. de Teresa, J. Pérez-Cacho, and M. R. Ibarra, Phys. Rev. B **62**, 5609 (2000).

[21] I. Dzyaloshinsky, J. Phys. Chem. Solids **4**, 241 (1958).

[22] T. Moriya, Phys. Rev. **120**, 91 (1960).

[23] A. S. Moskvin and I. G. Bostrem, Fiz. Tverd. Tela (Leningrad) **19**, 2616 (1977) [Sov. Phys. Solid State **19**, 1532 (1977)].

[24] This remains exactly valid if the orthorhombic lattice distortion is taken into account—i.e., if the x and y chains are not orthogonal.

[25] M. Tovar, G. Alejandro, A. Butera, A. Caneiro, M. T. Causa, F. Prado, and R. D. Sánchez, Phys. Rev. B **60**, 10199 (1999).

[26] V. Skumryev, F. Ott, J. M. D. Coey, A. Anane, J.-P. Renard, L. Pinsard-Gaudart, and A. Revcolevschi, Eur. Phys. J. B **11**, 401 (1999).

[27] J. Deisenhofer, M. V. Eremin, D. V. Zakharov, V. A. Ivanshin, R. M. Eremina, H.-A. Krug von Nidda, A. A. Mukhin, A. M. Balbashov, and A. Loidl, Phys. Rev. B **65**, 104440 (2002).

[28] E. Dagotto, T. Hotta, and A. Moreo, Phys. Rep. **344**, 1 (2001).

[29] T. Hotta, M. Moraghebi, A. Feiguin, A. Moreo, S. Yunoki, and E. Dagotto, Phys. Rev. Lett. **90**, 247203 (2003).

[30] K. Kubo, J. Phys. Soc. Jpn. **51**, 782 (1982).

[31] J. Zang, J. Zang, H. Röder, A. R. Bishop, and S. A. Trugman, J. Phys.: Condens. Matter **9**, L157 (1997).

[32] E. Dagotto, S. Yunoki, A. L. Malvezzi, A. Moreo, J. Hu, S. Capponi, D. Poilblanc, and N. Furukawa, Phys. Rev. B **58**, 6414 (1998).

[33] T. Nagamiya, in *Solid State Physics*, edited by F. Seitz, D. Turnbull, and H. Ehrenreich (Academic Press, New York, 1967), Vol. 20, p. 305.

[34] P.-G. de Gennes, Phys. Rev. **118**, 141 (1960).